HHS Public Access

Author manuscript

Cell Host Microbe. Author manuscript; available in PMC 2022 February 10.

Published in final edited form as:

Cell Host Microbe. 2021 February 10; 29(2): 210–221.e6. doi:10.1016/j.chom.2020.12.002.

Murine model of colonization with fungal pathogen *Candida auris* to explore skin tropism, host risk factors and therapeutic strategies

Xin Huang[1], **Charlotte Hurabielle**[2,†], **Rebecca A. Drummond**[3,‡], **Nicolas Bouladoux**[2,4], **Jigar V. Desai**[3], **Choon K. Sim**[1], **Yasmine Belkaid**[2,4], **Michail S. Lionakis**[3,*], **Julia A. Segre**[1,6,*]

[1]Microbial Genomics Section, National Human Genome Research Institute, NIH, Bethesda, Maryland 20892, USA.

[2]Metaorganism Immunity Section, Laboratory of Immune System Biology, National Institute of Allergy and Infectious Diseases, NIH, Bethesda, MD 20892, USA.

[3]Fungal Pathogenesis Section, Laboratory of Clinical Immunology and Microbiology, National Institute of Allergy and Infectious Diseases, NIH, Bethesda, MD 20892, USA.

[4]NIAID Microbiome Program, National Institute of Allergy and Infectious Diseases, Bethesda, MD 20892, USA.

Summary

Candida auris is an emerging multi-drug resistant human fungal pathogen. *C. auris* skin colonization results in environmental shedding, which underlies hospital transmissions, and predisposes patients to subsequent infections. We developed a murine skin topical exposure model for *C. auris* to dissect risk factors for colonization and to test interventions that might protect patients. We demonstrate that *C. auris* establishes long-term residence within the skin tissue compartment, which would elude clinical surveillance. The four clades of *C. auris*, with geographically distinct origins, differ in their abilities to colonize murine skin, mirroring epidemiologic findings. IL-17 receptor signaling and specific arms of immunity protect mice from long-term *C. auris* skin colonization. We further determine that commonly used chlorhexidine antiseptic serves as a protective and decolonizing agent against *C. auris*. This translational model

[*]Correspondence: lionakism@niaid.nih.gov (M.S.L.), jsegre@nhgri.nih.gov (J.A.S.).

Author Contributions

Conceptualization, M.S.L. and J.A.S.; Methodology, X.H., C.H., N.B. and C.K.S.; Formal Analysis, X.H. and M.S.L.; Investigation, X.H., C.H., R.D., N.B., C.K.S., and J.D.; Resources, Y.B., M.S.L., and J.A.S.; Data Curation, X.H., C.H., N.B., C.K.S., and J.D.; Writing – Original Draft, X.H., M.S.L., and J.A.S.; Writing – Review & Editing, X.H., C.H., R.D., C.K.S., J.D., Y.B., M.S.L., and J.A.S.; Visualization, X.H. and M.S.L.; Supervision, Y.B., M. S.L., and J.A.S.; Funding Acquisition, Y.B., M.S.L., and J.A.S.

[†]Present address: UCSF internal medicine, 505 Parnassus Avenue, San Francisco, CA 94143, USA

[‡]Present address: Institute of Immunology & Immunotherapy, College of Medical and Dental Sciences, University of Birmingham, Birmingham, B15 2TT, UK

[6]Lead Contact

Declaration of Interests

The authors declare no competing interests.

facilitates an integrated approach to develop strategies to combat the unfolding global outbreaks of *C. auris* and other skin-associated microbial pathogens.

Graphical Abstract

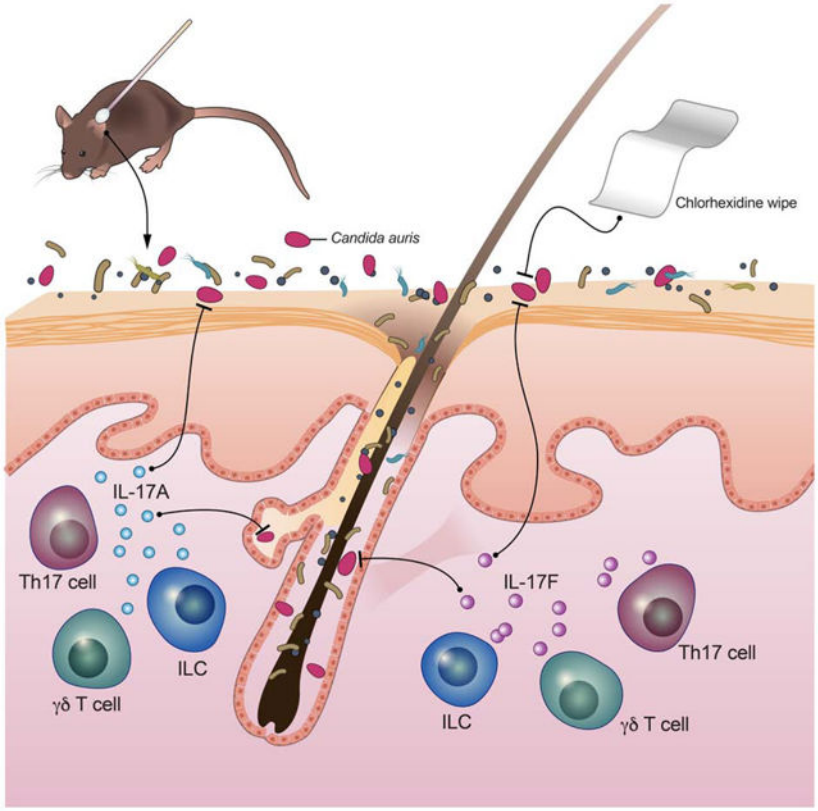

In Brief

The mechanisms by which *Candida auris*, an emerging human fungal pathogen, colonizes skin remain largely uncharacterized. Using a translational model, Huang et al. demonstrate within tissue residence by *C. auris*, and reveal that IL-17 signaling provides protection against *C. auris* both on the skin surface and within skin tissue.

Keywords

Candida auris; fungal pathogen; skin colonization; epidemiology; translational mouse model; adaptive and innate immunity

Introduction

The human-associated fungal pathogen *Candida auris* has emerged as a serious threat to global health because of its high rates of evolved antimicrobial resistance, high mortality associated with bloodstream infection and high transmission rates within healthcare facilities (https://www.cdc.gov/fungal/candida-auris) (Lockhart et al., 2017). *C. auris* was first

identified in 2009 from a clinical culture of a Japanese patient's external ear canal (Satoh et al., 2009) and in the ensuing decade, multiple outbreaks of skin colonization and/or associated bloodstream infection have occurred globally with an associated mortality rate of up to 60% (Forsberg et al., 2019). *C. auris* is one of only five microbial pathogens with the highest rating of urgent threat in the 2019 antibiotic resistance report released by the US Centers for Disease Control and Prevention (CDC) (CDC, 2019). Both the CDC (https://www.cdc.gov/fungal/candida-auris/candida-auris-alert.html) and Public Health England (https://www.gov.uk/government/publications/candida-auris-emergence-in-england/candida-auris-identified-in-england) issued multiple clinical alerts about *C. auris*. Within the United States, *C. auris* was made nationally notifiable in 2018 with over 1,000 cases reported to date. Over one million invasive fungal infections occur globally, increasingly from multi-drug resistant *C. auris* (Lionakis and Hohl, 2020). The advancement of medical technologies, such as organ and bone marrow transplantation, has also exposed more patients to nosocomial fungal infections

Many of the proposed factors for *C. auris* skin colonization and bloodstream infection co-occur in vulnerable hospitalized patients who are at risk for acquisition of nosocomial infections, thus, delineating primary drivers of patient susceptibility has been challenging (Vallabhaneni et al., 2019). Approximately half of the *C. auris* clinical cases in the United States have been in the bloodstream, but skin sites (axilla, groin) are considered the primary sites of asymptomatic colonization (Vallabhaneni et al., 2016). Colonization is distinct from infection as it typically results in asymptomatic carriage; however, skin colonization often precedes and is a risk factor for subsequent bloodstream infection. Hence, identifying *C. auris* colonized patients is a crucial component of infection control because these patients are at increased risk for developing a subsequent bloodstream infection, and pose a risk for nosocomial transmission to other patients in the ward.

C. auris has been demonstrated to colonize the skin of patients for months, and to persist as viable in the environment for weeks (Adams et al., 2018; Welsh et al., 2017), which both likely contribute to the nosocomial transmission of *C. auris*. Indeed, an investigation of a *C. auris* outbreak in an intensive care unit identified *C. auris*-bearing reusable skin-surface axillary temperature probes as a mode of nosocomial transmission (Eyre et al., 2018). Persistence on the skin and in the environment are unique features for *C. auris* which have not been observed with other *Candida* species that cause human infections, such as *Candida albicans* or *Candida glabrata*, which more typically reside within the human gastrointestinal tract.

Given the remarkable propensity of *C. auris* to colonize the human skin for prolonged periods of time, employing infection control measures for curtailing patient skin colonization by *C. auris* and preventing nosocomial transmission represents a major unmet medical need. To that end, bathing patient skin with the common antiseptic chlorhexidine gluconate (CHG) has increasingly become standard of care to reduce multi-drug resistant (MDR) bacterial transmission and infection (Huang et al., 2013; Huang et al., 2019a) and may represent a viable strategy to combat *C. auris* skin colonization in humans. However, this hospital practice has raised some concerns that CHG might deplete the commensal microbiota which provide colonization resistance and/or induce resistance among pathogens

(Kampf, 2016), such as *C. auris*. Therefore, defining the efficacy of CHG in preventing or eliminating colonization by *C. auris* in preclinical models *in vivo* has important clinical implications.

Whole-genome sequencing and epidemiologic investigations have revealed near simultaneous emergence of genetically distinct clades of *C. auris* on different continents: East Asia, South Asia, South America, and Africa (Lockhart et al., 2017), with a potential fifth Iranian clade (Chow et al., 2019). The clades differ by tens to hundreds of thousands of DNA base pairs, but isolates are highly clonal within each clade (Chow et al., 2018). The simultaneous emergence of multiple phylogenetically distinct geographic clades presenting with high levels of antimicrobial resistance and causing disease among patients worldwide remains an epidemiologic enigma (Chow et al., 2020).

Previous studies examined the pathogenicity of systemically introduced *C. auris* infection in murine (Ben-Ami et al., 2017; Torres et al., 2019; Xin et al., 2019) and insect (Wurster et al., 2019) models. However, thus far, no animal model has been developed to examine fungal and host determinants of *C. auris* skin colonization. Here, we report a mouse model for *C. auris* skin colonization to facilitate translational research into features of human disease. We employ a series of studies to explore the underlying biology of *C. auris* as a human-associated pathogen, dissect risk factors for colonization and test preventive and therapeutic strategies which may be adopted to protect patients. This model provides the foundation for enhancing our understanding of fungal virulence traits, protective host immune responses, *in vivo* fitness of multi-drug resistant (MDR) strains, infection control interventions, and effective treatment modalities against *C. auris* skin colonization. This translational mouse model of skin colonization and evaluation of infection control measures could be adapted for other MDR microbes, such as Gram-negative and Gram-positive bacteria, which colonize the skin and cause life-threatening infections in hospitalized patients.

Results

Candida auris Persistently Colonizes Skin

To model epidemiologic features of nosocomial transmission, we extended our previously reported skin microbial colonization mouse model (Naik et al., 2015) and applied *C. auris* topically to the skin surface of the ear pinnae and shaved back (Figure 1A) of immunocompetent wild-type (WT) C57BL/6NTac mice. This model of skin colonization in the context of existing normal microbial communities has previously been used to demonstrate how tissue-resident immune cells are poised to sense and respond to alterations in microbial communities (Naik et al., 2015). In keeping with clinical relevance, the clinical isolate recovered from an NIH *C. auris*-infected patient (Vallabhaneni et al, 2016), which belongs to the South Asian clade, was used in most experiments in this study, unless noted otherwise.

To delineate body site tropism of fungi within the *Candida* genus, we compared fungal load on the skin and in the gut of mice colonized by *C. auris* and *C. albicans* over two weeks. Through mouse grooming behavior, fungal cells topically applied to mouse skin entered the gastrointestinal tract. At the 2-week endpoint, modeling the duration of a typical patient

hospital stay, *C. auris* consistently colonized the skin surface of WT mouse ear pinnae (determined by swabbing), whereas *C. albicans* minimally colonized WT mouse ear skin (Figures 1A and 1B). Strikingly, higher concentrations of *C. auris* resided deeper within the skin (determined by disaggregation of tissue), whereas *C. albicans* did not reside within the skin tissue compartment (Figure 1B). Colonies, grown on selective media, were confirmed as *C. auris* with species-specific PCR primers (data not shown). As expected, *C. albicans* only sporadically colonized the WT mouse intestinal tract with very rare examples of *C. auris* intestinal colonization (Figure 1B).

Human patients are screened for *C. auris* colonization with non-invasive swabs of the skin surface. However, in the murine model following topical association, *C. auris* cells were observed both on the skin surface and deeper inside the tissue, resident within the hair follicle (Figure S1A). To test whether skin tissue could serve as an unrecognized reservoir for *C. auris* colonization, we examined persistence of *C. auris* residence on the surface and deeper within the skin tissue compartment. After topical association with *C. auris*, WT mice were examined for surface colonization on a weekly basis to model clinical epidemiologic surveillance. Skin surface swabs were negative 50 days after initial *C. auris* colonization in all 16 mice tested. At the same time, we recovered *C. auris* from deeper skin tissue in 3 of 4 mice tested (Table S1). With monthly surveillance, we continued to recover live *C. auris* colonies from deeper skin tissue for up to 4 months after initial colonization, which is two months after the mouse would have been considered ‘clear’ of *C. auris* skin colonization based on surface swabbing (Table S1). While *C. auris* colonization deeper in tissue has not been explored in human patients due to the risk of performing invasive sampling, it might potentially explain the clinical observation of skin surface surveillance cultures that grow out *C. auris* after multiple prior negative results.

Clinical reports have suggested that broad-spectrum antibiotic or azole antifungal pre-exposure and diabetes may be associated with *C. auris* colonization and/or infection (Khan et al., 2018; Lockhart et al., 2017; Parra-Giraldo et al., 2018). However, those features are common in patients with prolonged hospitalization and it is currently unknown if they increase the risk of developing *C. auris* colonization and infection. We utilized our model of *C. auris* skin association to examine the direct impact of broad-spectrum antibiotic pre-exposure (Kobayashi et al., 2015), fluconazole pre-exposure, diabetes (Grice et al., 2010), and high-fat diet (Ridaura et al., 2018), all of which are known to alter the skin microbiome and to affect topical host immune responses against microbes, on *C. auris* skin colonization. Notably, we found no increase in *C. auris* skin colonization in any of these conditions (Table S2), indicating that these factors may not directly predispose to skin *C. auris* colonization. Future studies will be needed to investigate whether the combination of these factors can contribute to higher *C. auris* burden on the skin.

In addition to their distinct genetic differences and geographic origins, the four clades of *C. auris* are reported as having differences in antimicrobial resistance, colonization and transmission rates (Chow et al., 2018). To assess if the clades feature intrinsic genetic differences that may account for their differential clinical manifestations, we tested the four clades in our murine skin colonization model. Mirroring reported epidemiologic features, the four clades of *C. auris* colonized WT skin at different levels. Specifically, two weeks after *C.*

auris exposure, the African clade led to the highest topical skin colonization, with similar albeit lower rates of skin colonization observed for the South American, South Asian and East Asian clades (Figure 1C). In keeping with the paucity of outbreaks reported for the East Asian clade, this clade colonized WT mouse skin at lower levels (Figure 1C). Demonstrating the long-term risk for persistent and potentially undetected colonization, all *C. auris* clades became resident within the skin tissue, with the highest rate observed for the African clade and the lowest rate observed for the South Asian and East Asian clade (Figure 1D).

Previous studies that utilized a single clade suggested that *C. auris* was less virulent than *C. albicans* in a mouse model of disseminated candidiasis when introduced systemically into WT mice. Indeed, neutropenia and/or corticosteroid administration were essential in those studies to elicit lethality in *C. auris*-infected mice whereas *C. albicans* is known to cause lethality in immunocompetent WT mice upon intravenous inoculation (Ben-Ami et al., 2017; Lionakis and Netea, 2013; Torres et al., 2019; Wang et al., 2018). This inter-species difference may relate to the ability of *C. albicans*, and not *C. auris*, to filament *in vivo*, a critical determinant of renal injury and lethality in the mouse model of disseminated candidiasis (Ben-Ami et al., 2017; Lionakis and Netea, 2013). Because differential fungal strain and clade virulence have been documented for *C. albicans* in the systemic infection model (Marakalala et al., 2013), we explored whether any of the four clades of *C. auris* that effectively colonize the mouse skin would induce lethality upon systemic inoculation in WT mice, and used the virulent *C. albicans* SC5314 strain as a positive control. As expected, intravenous injection of 10^5 *C. albicans* cells resulted in mortality for all mice by day 30 post injection (Figure S2). By contrast, none of the four clade strains of *C. auris* resulted in similar rates of mortality, with only a single mouse, inoculated with the African clade, succumbing during the 30-day study. Taken together, these results demonstrate an intrinsic tropism for skin colonization by *C. auris*, with deeper skin residence as a potential reservoir for the pathogen and provide a model of experimental *C. auris* skin colonization with translational relevance.

Skin Association with *C. auris* Promotes a Protective IL-17A/IL-17F Response Derived from Innate and Adaptive Lymphoid Cells

As previously shown with commensal bacterial topical application (Naik et al., 2015; Naik et al., 2012), skin association with *C. auris* did not appear to cause overt skin inflammation or disruption of the skin architecture as evidenced by the absence of skin erythema or histological evidence of hyperkeratosis or spongiosis (Figure S1B-D). *C. auris* topical association resulted in the accumulation of $CD4^+$ T cells and $CD8^+$ T cells, but not γδ T cells or innate lymphoid cells (ILCs) (Figure 2A). Among T helper subsets, *C. auris* topical association led to a selective accumulation of $CD4^+$ IL-$17A^+$ and $CD4^+$ IL-$17F^+$ (Th17) cells within the skin compartment (Figures 2B, 2C and S3), without expansion in skin Th1 (CD4+IFN-g+), Th2 (CD4+IL-5+), regulatory T (CD4+Foxp3+) cells (Figures S3 and S4A-C). *C. auris* topical application also promoted the accumulation of IL-17A- and IL-17F-producing $CD8^+$ T cells (Tc17), IL-17A-producing γδ T cells, and IL-17A-producing ILCs (Figures 2B, 2C and S3) within the skin.

IL-17 receptor (IL-17R) signaling is well-recognized to play an indispensable role in mucocutaneous host defense against fungi (including *Candida* species) in mice and humans (Boisson et al., 2013; Conti et al., 2016; Lionakis and Levitz, 2018; Puel et al., 2011). Hence, we next asked whether the observed induction of an IL-17A/IL-17F response in *C. auris*-associated skin is protective against fungal skin colonization. We applied *C. auris* topically on the skin of mice deficient in the IL-17R-associated adaptor molecule Act1, which lack IL-17R-dependent cellular responses (Sonder et al., 2011), and recovered significantly increased amounts of *C. auris* from the *Act1*$^{-/-}$ mouse skin surface, skin tissue compartment, and intestinal luminal content (Figures 2D and 2E). Deficiency of the type 17-associated cytokine IL-22 was dispensable for the control of *C. auris* skin colonization as shown by experiments in both *Il22*$^{-/-}$ mice and *Act1*$^{-/-}$ mice in which IL-22 was neutralized using an antibody-based approach (Figure S4D-F). Collectively, these data indicate that skin association with *C. auris* drives an IL-17A-IL-17F/IL-17R response which promotes the control of *C. auris* skin colonization.

Previous studies have shown that induction of *C. albicans*-specific Th17 cells in the skin relies on Langerhans cells while induction of IL-17 at early time points post-*C. albicans* exposure is mediated by CD301b^{+} dermal dendritic cells (Igyarto et al. 2011; Kashem et al. 2015). Mice deficient in Langerhans cells (Lan-DTA) controlled *C. auris* skin colonization normally (Figure S4G). These data suggest that Langerhans cells may not be implicated in the overall cutaneous IL-17 response to *C. auris*, as it has been reported for *C. albicans* (Igyarto et al. 2011; Kashem et al. 2015). Moreover, the C-type lectin receptor adaptor molecule Card9 has been shown to promote the induction of Th17 cells upon systemic or oropharyngeal *C. albicans* infection and upon cutaneous *Malassezia* challenge, but it is dispensable for the development of innate type 17 responses in the setting of oropharyngeal candidiasis and skin *Malassezia* infection (LeibundGut-Landmann et al., 2007; Bishu et al., 2014; Kashem et al., 2015; Sparber et al. 2019). Mice deficient in Card9 controlled *C. auris* skin colonization in a similar manner to WT mice, suggesting that C-type lectin receptor signaling may not be implicated in the overall cutaneous IL-17 response to *C. auris* (Figures S4H).

To explore further the relative contribution of IL-17A/IL-17F derived from innate and/or adaptive lymphoid cells in protection against *C. auris* skin colonization, we next applied *C. auris* topically on the skin of *Rag2*$^{-/-}$ mice, which lack αβ and γδ T cells, and *Rag2*$^{-/-}$*Il2rg*$^{-/-}$ mice, which also lack ILCs. With *C. auris* colonization, *Rag2*$^{-/-}$ mice exhibited enhanced accumulation of IL-17A and IL-17F producing ILCs in the skin relative to WT mice (Figure 3A). While *Rag2*$^{-/-}$ mice had greater *C. auris* skin colonization than WT mice, *Act1*$^{-/-}$ mice exhibited even greater *C. auris* skin colonization (Figures 2D and 3B). Of note, we found significantly increased *C. auris* colonization on the skin surface, deeper within the skin tissue, and in the intestinal luminal content of *Rag2*$^{-/-}$*Il2rg*$^{-/-}$ mice (Figure 3C), which persisted for several months following the initial skin association with *C. auris* (Figures 3D and 3E). When comparing the degree of *C. auris* skin colonization in *Rag2*$^{-/-}$ versus *Rag2*$^{-/-}$*Il2rg*$^{-/-}$ mice, *Rag2*$^{-/-}$*Il2rg*$^{-/-}$ mice exhibited ~1 log greater CFU on the skin surface and deeper within the skin tissue (Figures 3B and 3C). Together these experiments suggest that production of IL-17A/IL-17F by a combination of αβ T cells, γδ T cells and ILCs contributes to the control of *C. auris* colonization. Future studies will be needed to

define potential immune factors derived from innate and adaptive lymphoid cell subsets other than IL-17A/IL-17F that may confer protection against *C. auris* colonization in the model. Histological examination of the *C. auris*-associated skin of *Rag2*$^{-/-}$*Il2rg*$^{-/-}$ mice using Grocott-Gomori's methenamine silver stain revealed clusters of *C. auris* on the skin surface as well as deeper in the skin compartment within the hair follicle structure (Figures 3F and 3G). Clusters of Grocott-Gomori's methenamine silver stained cells in naïve WT mice were not observed (data not shown).

Chlorhexidine Gluconate Protects WT Mice from *C. auris* Colonization and Helps Decolonize *Rag2*$^{-/-}$*Il2rg*$^{-/-}$ mice

Given *C. auris*' high levels of antimicrobial resistance against multiple classes of antifungal drugs (i.e., azoles, polyenes, echinocandins), treatment options for *C. auris* bloodstream infection are limited (Larkin et al., 2017; Singh et al., 2019), especially with pan-resistant *C. auris* isolates recently reported in the United States (Ostrowsky et al., 2020). Limited therapeutic modalities underscore the essential role for effective infection control measures to prevent hospital transmission and bloodstream infections. The antiseptic CHG is commonly used to care for the skin of patients in hospitals and nursing homes as it has demonstrated effectiveness in reducing rates of MDR bacterial transmission and infection (Huang et al., 2019a). However, as *C. auris* outbreaks have occurred in facilities with established CHG bathing procedures, concern has been raised that CHG might be depleting the natural skin microbial shield allowing *C. auris* to persist on the skin and/or cause infections.

To disentangle CHG bathing from other concurrent epidemiologic risk factors seen in patients, we utilized our mouse model to explore the impact of CHG on *C. auris* skin colonization. CHG wipes, similar to those used on human skin, were used to 'bathe' the mouse skin daily for four days before *C. auris* topical association (Figure 4A), to mimic the effect of prophylactic use of CHG before patient exposure to *C. auris*. Next, to mimic the range of fungal exposures in healthcare facilities (Zhu et al., 2019), 10^7 and 10^9 CFUs of *C. auris* was topically applied to the skin of WT mice. CHG had a protective effect against *C. auris* skin colonization in both concentrations of applied *C. auris*, with complete eradication of skin colonization at the lower exposure concentration of 10^7 *C. auris* (Figure 4B). CHG treatment also prevented *C. auris* from establishing residence within the skin tissue compartment, again completely eliminating skin colonization at the lower exposure concentration of 10^7 *C. auris* (Figure 4C).

Furthermore, to test whether CHG was effective at promoting decolonization of *C. auris* from colonized mouse skin, and to mimic the effect of CHG after patient exposure to *C. auris*, *Rag2*$^{-/-}$*Il2rg*$^{-/-}$ mice (which were shown above to exhibit greater and persistent *C. auris* colonization in the skin) were first exposed to *C. auris* and then subsequently their skin was cleaned daily with CHG wipes (Figure 4D). Demonstrating its effectiveness, CHG reduced the *C. auris* load, both on the mouse skin surface and within the skin tissue compartment (Figures 4E and 4F). Together, these experiments demonstrate the effectiveness of CHG in preventing and ameliorating preexisting *C. auris* skin colonization

and provide the basis for evaluating the efficacy of CHG in reducing the risk of subsequent infection and nosocomial transmission in the clinical setting.

Clinical microbiology laboratories are increasingly using quantitative PCR (qPCR)-based assays with *C. auris* specific primers to test surveillance skin swabs. A previous study demonstrated that CHG retains bacterial DNA on mouse skin (SanMiguel et al., 2018). We therefore sought to test whether CHG retained *C. auris* genomic DNA (gDNA) on mouse skin, which could have important implications for epidemiologic surveillance. Following an initial topical association with *C. auris*, the skin of mice was wiped every other day with either CHG or PBS as a control. During this time, skin swabs were taken every four days for both culture- and qPCR-based detection of *C. auris*. While *C. auris* load on the skin surface decreased over time on the skin of both CHG-exposed and control mice as determined by culture, the qPCR cycle threshold (Ct) values were consistently 2 cycles lower in the CHG group compared with control (Table S3). Since the levels of live (cultivable) *C. auris* were declining in CHG and control mice, the lower qPCR results in CHG mice likely represents PCR amplification from dead or compromised cells. Paradoxically, while CHG reduced the burden of live *C. auris* skin colonization, monitoring *C. auris* colonization levels solely with qPCR would have demonstrated an increased level of *C. auris* gDNA. These experiments underscore the need for clinical tests to benchmark molecular assays to culture based assays for hospital infection control.

Discussion

Over the last decade, *C. auris* has emerged simultaneously as four distinct genetic and geographic clades, with its origin still very much a mystery (Jackson et al., 2019). This MDR fungal pathogen is already causing global outbreaks that are difficult to control and are associated with significant healthcare-associated costs, as exemplified by one outbreak which required the facility to shut down for several months to eradicate the pathogen. Due to the paucity of antifungal treatment options for increasingly resistant *C. auris* bloodstream infections, effective infection control approaches are urgently needed to thwart the pathogen from spreading. Unlike other Candida species, *C. auris*' unique ability to persist on human skin and in the hospital environment requires new biological insights into the host-pathogen life cycle. Our study presents a translational murine skin colonization model for *C. auris* which we employed to investigate risk factors for *C. auris* skin colonization, and to test infection control measures. Strikingly, we discover that *C. auris* is able to reside deep within the skin tissue compartment for months after skin surface swabs are repeatedly negative. Herein, we utilized the model to reveal a differential *C. auris* clade-specific propensity to persist in the skin, to define a clinically relevant immune deficiency state that predisposes to *C. auris* skin colonization, and to show that CHG can act as a protective and decolonizing agent against *C. auris*.

Previous studies have established various immunodeficient models for systemic *C. auris* infection in inbred mouse strains in the setting of neutropenia, corticosteroid use or chemotherapy administration (Ben-Ami et al., 2017; Torres et al., 2019; Xin et al., 2019). On the other hand, immunocompetent mice can survive high inocula of *C. auris* bloodstream challenge (Torres et al., 2019; Wang et al., 2018), with an exception of one study that used

outbred ICR immunocompetent mice and showed lethality after *C. auris* challenge (Fakhim et al., 2018). Our results in immunocompetent C57BL/6NTac mice are consistent with most previous studies, in that intravenous challenge of a dose sufficient to kill *C. albicans*-infected mice does not pose a lethal threat to *C. auris*-challenged mice. Hence, *C. auris* appears to behave in this systemic model similar to *C. glabrata*, another medically important *Candida* species that does not result in *in vivo* filamentation or mouse lethality, yet it accounts for a significant and increasing proportion of human infections (Pappas et al., 2018). The fact that *C. auris* is primarily a skin colonizer underscores the difficulty in controlling the spread of the pathogen in healthcare settings (Ruiz-Gaitan et al., 2018). It is therefore likely that *C. auris* can colonize the patient skin long-term, and cause harm once it enters the bloodstream through breach of the mucocutaneous barriers in the setting of surgery or central venous catheters, and/or in the setting of underlying immune deficiency conditions of the patient.

Our surprising finding that *C. auris* resides within the mouse ear tissue long-term is indicative of potential major challenges in controlling *C. auris* in human populations. In our study, we occasionally observed re-emergence of *C. auris* on mouse skin that had been skin surface negative by culture several days prior. A previous clinical study had similarly observed the re-emergence of *C. auris* on patient skin after three consecutive negative culture screens (Eyre et al., 2018), suggesting that a skin tissue reservoir for *C. auris* may exist in humans, as in mice. Residence of *C. auris* within the skin tissue compartment might lead to bloodstream infection and its re-emergence on the skin surface could re-initiate hospital transmission, especially if infection control measures have meanwhile been withdrawn given prior consecutive negative skin surface culture screens. Our findings of a skin tissue reservoir of *C. auris* in our translational model and the early clinical reports are suggestive of such a reservoir in humans (Schelenz et al., 2016). However, directly testing humans for skin tissue residence of *C. auris* using punch biopsies is not advisable due to its invasive nature. Understanding how to deplete or deprive *C. auris* of this deeper tissue residence may prove critical for devising successful decolonization strategies in patients.

Our results that the four clades of *C. auris* differentially colonize the WT mouse skin are consistent with clinical observations that the East Asian clade is rarely implicated in outbreaks in human patients, unlike other clades (Jackson et al., 2019). As genetic tools are developed to manipulate the *C. auris* genome, future studies will explore the underlying differences that contribute to African, South Asian and South American clades' proclivity for skin commensalism relative to the East Asian clade (Chow et al., 2020).

We found that *C. auris* skin colonization triggers an IL-17A$^+$ and IL-17F$^+$ response by several lymphoid cell populations, similar to the response elicited by *C. albicans* skin association (Kashem and Kaplan, 2018; Harrison et al., 2019). Interestingly, extending the well-recognized contribution of IL-17R signaling in mucocutaneous host defense in mice and humans (Boisson et al., 2013; Conti et al., 2016; Lionakis and Levitz, 2018; Puel et al., 2011), Act1 deleted mice, deficient in the IL-17 pathway, had a higher *C. auris* burden on the skin surface, skin tissue compartment and gut compared with WT mice. These results suggest that a competent IL-17R pathway contributes to keeping *C. auris* in check on the skin surface and tissue likely via facilitating the production of antifungal antimicrobial peptides by keratinocytes and promoting cutaneous barrier integrity and function. This

finding has important translational implications because IL-17R-targeted biologics have been increasingly used in patients with autoimmune conditions such as psoriasis and inflammatory bowel disease (Frieder et al., 2018) and have been associated with mucocutaneous candidiasis in such patients (Saunte et al., 2017), which might also predispose them to greater and/or prolonged *C. auris* skin colonization. As well, other immunomodulatory agents such as corticosteroids can down-regulate IL-17R responses (Guggino et al., 2015), which could be a risk factor for greater and/or prolonged *C. auris* skin colonization in corticosteroid-treated patients. Of note, prior corticosteroid exposure has commonly been reported in patients with *C. auris* infection (Khan et al., 2018; Lockhart et al., 2017; Parra-Giraldo et al., 2018), making it plausible that corticosteroids may contribute to *C. auris* skin colonization via impaired IL-17A/IL-17F responses in the skin. Future studies will be needed to directly examine this hypothesis in the mouse model. Importantly, we show that both innate and adaptive lymphoid cellular sources of IL-17A/IL-17F appear to contribute in curtailing *C. auris* skin colonization as $Rag2^{-/-}Il2rg^{-/-}$ mice, and to a lesser extent $Rag2^{-/-}$ mice, exhibited greater *C. auris* skin colonization. This finding supports the notion that deficiency of IL-17 production by a given cell population can be, at least partially, compensated at the mucocutaneous barrier by other IL-17-producing cells to promote IL-17R response competency. Taken together, these results suggest a specific clinically relevant immune deficiency as a risk factor for *C. auris* skin colonization. In addition, this work provides the basis for further investigations aiming to uncover other IL-17-independent immune factors produced by αβ T cells, γδ T cells, ILCs, and other immune and non-hematopoietic cells that may also regulate *C. auris* skin colonization.

CHG is typically used as an antiseptic in a wide range of healthcare settings. CHG has been tested extensively in humans and it is safe and effective against Gram-positive and Gram-negative bacteria and yeasts (Septimus and Schweizer, 2016). Increasingly, long-term acute care hospitals and skilled nursing facilities are adopting daily CHG bathing for their patients, although concerns have been raised about development of acquired resistance to CHG among bacterial pathogens (Kampf, 2016). A previous study indicated that CHG might disrupt the commensal bacterial communities on patient skin (Cassir et al., 2015). However, a more recent study appears to reach different conclusions (Kates et al., 2019). Importantly, topical CHG combined with nasal mupirocin has proven effective in reducing overall bloodstream infections for patients with medical devices (Huang et al., 2019a), and also in reducing postdischarge infection rates for methicillin-resistant *Staphylococcus aureus* (Huang et al., 2019b). Previous *in vitro* tests indicate at most 2 orders of magnitude reduction against *C. auris* growth by CHG (Rutala et al., 2019). Our *in vivo* study demonstrates the protective effect of CHG against *C. auris* colonization for both skin surface and skin tissue residence in mice by *C. auris*. This murine model supports the use of CHG bathing to protect patients from *C. auris* skin colonization, but this requires formal clinical trial testing.

Protocols to culture *C. auris* from surveillance or clinical samples require one-week growth, which is not practical for infection control in patients. Therefore, clinical microbiology laboratories are increasingly relying on qPCR-based results as the initial screen. We demonstrated that CHG trapped *C. auris* gDNA on the mouse skin, beyond the time point that live fungi could be recovered by culture. This discrepancy between molecular- and the

culture-based assays might generate contradictory results regarding CHG's ability to increase or decrease *C. auris* skin colonization, respectively. Future studies in *C. auris*-colonized patients will be required to directly compare the performance of qPCR- and culture-based assays in detecting *C. auris* biomass and viability on the human skin.

In summary, we have developed a murine model of *C. auris* skin colonization with translational relevance that demonstrates *C. auris*' tropism for long-term skin colonization and provides a tractable *in vivo* system for the testing of *C. auris* virulence traits, host immune responses, the role of clinical risk factors (e.g., antibiotic pre-exposure, antifungal pre-exposure, diabetes), infection control measures and treatment approaches against this emerging MDR fungal pathogen of human patients.

STAR * Methods

RESOURCE AVAILABILITY

Lead contact—Further information and requests for reagents may be directed to and be fulfilled by the corresponding authors, Michail S. Lionakis (lionakism@niaid.nih.gov) and Julia A. Segre (jsegre@nhgri.nih.gov).

Materials Availability—Experimental models (organisms, strains) generated for use in this study will be made available on request, but we may require a completed Materials Transfer Agreement if there is potential for commercial application. These materials are available for distribution under the Uniform Biological Material Transfer Agreement, a master agreement that was developed by the NIH to simplify transfers of biological research materials.

Data and Code Availability—The published article includes all datasets generated or analyzed during this study . This study did not generate any unique datasets or code

EXPERIMENTAL MODEL AND SUBJECT DETAILS

Animal Studies—Wild-type (WT) and immunodeficient mice used in this study were female C57BL/6 mice at 8-10 weeks of age, unless specified below. *Rag2*$^{-/-}$ and *Rag2*$^{-/-}$*Il2rg*$^{-/-}$ mice were on the C57BL/10 background, with age and sex matched WT C57BL/10 as controls. Male *Il22*$^{-/-}$ and Langerhans cell deficient (Lan-DTA) mice were used with appropriate controls. All mice were healthy before initiation of studies, were not subjected to previous procedures, and were naive to drugs. All mice were maintained in an SPF environment at an American Association for the Accreditation of Laboratory Animal Care (AAALAC)-accredited animal facility at the NIAID and housed in accordance with the procedures outlined in the Guide for the Care and Use of Laboratory Animals. All experiments were performed at the NIAID under an animal study proposal approved by the NIAID Animal Care and Use Committee, in a BSL-2/3 room with necessary precaution for working with *Candida auris*. Mice were provided with water and a standard laboratory diet *ad libitum* except if noted otherwise. They were supplied with hardwood chips as bedding and housed in a temperature-controlled, air-conditioned room on a 12-hr light-dark cycle.

All mice were co-housed at 5 mice maximum in each cage. Animals were assigned randomly to experimental groups.

Fungi—Stocks of *Candida albicans* (SC5314) and *Candida auris* (various clades) were streaked out on Sabouraud dextrose agar with chloramphenicol and incubated at 37°C for at least two days. Single colonies were grown with shaking overnight (220 rpm) at 30°C in Yeast Extract-Peptone-Dextrose (YPD).

METHOD DETAILS

Murine skin colonization model—One or two days before topical association, mouse dorsal hairs were shaved to provide easy access to the back skin. For skin colonization experiments, fungi were cultured, as described above, washed once with PBS, and resuspended at a concentration of $5x10^9$ yeasts/mL of PBS unless otherwise noted. Individual mice were topically associated with $1x10^9$ yeast cells on the shaved dorsal skin and pinna areas using a Puritan cotton swab every other day two (chlorhexidine experiments) or four times (all other experiments).

At defined time points, skin surface was swabbed and on day 14, skin swabs, skin tissue and intestinal content were taken, weighed and processed for culturing as described below. Experiments performed using this two-week model include: comparing *C. auris* with *C. albicans* for skin and gut colonization in WT mice; comparing skin colonization between different *C. auris* clades, i.e., East Asian (CDC # 0381), African (CDC # 0383), South American (CDC # 0385), South Asian (CDC # 0387) and NIH; comparing WT with genetically defined mouse models, including *Rag2*$^{-/-}$, *Rag2*$^{-/-}$*Il2rg*$^{-/-}$, *Card9*$^{-/-}$, *Il22*$^{-/-}$ and Lan-DTA mice.

Quantification of fungal load on mouse skin surface, within skin tissue and intestinal content—Skin surface swabs were taken periodically from dorsal and pinna skin using BD eSwab (moistened in sterile PBS prior to sampling) and placed in transport media. Skin swabs were processed as described in (Welsh et al., 2017) with both direct and enrichment cultures. Briefly, after 10 seconds of vigorous vortexing, 75 µl of the initial transport medium, plus the media on the cotton head, was plated on a CHORMagar Candida plate, and incubated at 37°C for up to one week. Separately, 150 µl of the transport medium was pipetted into a 14 ml round bottom tube with 2.5 ml of enrichment broth (Sabouraud dextrose broth with 10% Sodium Chloride and 50 mg/l chloramphenicol and gentamycin, pH 5.6±0.2). Tubes were incubated with shaking at 37°C for a week, before 100 µl of broth was plated on a CHORMagar *Candida* plate and incubated overnight at 37°C. For both direct and enrichment cultures, pink colonies, indicating *C. auris*, were verified with species specific PCR (Figure S1) and counted. To calculate the number of colony forming units (CFUs), colonies from direct plating were utilized. However, if direct plating demonstrated no growth, then the enrichment broth culture plate was examined for possible low level positivity and this number was utilized to calculate CFU.

For investigations of resident skin tissue colonization, ear sheets were separated and dorsal skin slices cut into 2-3 smaller pieces. Tissue was digested in RPMI containing 100 U/ml penicillin, 100 µg/ml streptomycin, 1 mM sodium pyruvate, 1x MEM nonessential amino

acid solution, 20 μM HEPES, and 0.25 mg/ml Liberase TL or 2.5 mg/ml collagenase D by incubating for 1 hour and 45 minutes at 37°C and 5% CO_2. Digested skin sheets were homogenized using a Medicon/Medimachine tissue homogenizer system. Liberated cells were suspended in approximately 2.5 ml (for pinna sheets) or 2 ml (for dorsal skin) RPMI media plus 3% fetal bovine serum. 250 μl of the suspension was plated on CHORMagar plates. Limit of detection is 40 CFU/g of skin tissue.

Cecal contents were obtained by making a cut along the cecal pouch and homogenizing contents in 3ml sterile PBS. Contents of small intestine were flushed out with PBS using a syringe and oral gavage tube and homogenized in 3ml sterile PBS. Colonic contents were extracted by pinching the colon with forceps and gently nudging out the contents, which were homogenized in 1.2ml sterile PBS. 250 μl of the suspension was plated on CHORMagar plates. Limit of detection is 20 CFU/g of gastrointestinal content.

PCR confirmation for selected colonies recovered from skin swabs, disaggregated skin tissue and intestinal content—To confirm the identity of the fungi cultured, select pink colonies from CHORMagar *Candida* plates were stored in YPD medium with 20% glycerol at −80°C. Each colony was tested using the following reaction: 10 μl of 2x Qiagen Hot Start Pre-mix, 1 μl of 10 μM *C. auris* species specific (Kordalewska et al., 2017) primers [CauF 5'-CGCACATTGCGCCTTGGGGTA-3' and CauR 5'-GTAGTCCTACCTGATTTGAGGCGAC-3'], 4 μl of thawed out colony stock and 5 μl of PCR water. The PCR profile started with 5 minutes at 95°C, followed by 30 cycles of 30 seconds at 95°C, 30 seconds at 55°C and 1 minute at 72°C, ending with 10 minutes at 72°C. *C. auris* genomic DNA (gDNA) was included as a positive control and water as the negative control.

Long-term residence within ear skin tissue by *C. auris* in WT mice—Four cages, each with four WT mice, were set up in parallel and colonized four times on every other day. After all mice turned skin surface negative by swabbing (day 50), one mouse from each cage was sacrificed on a monthly basis (days 58, 98, 120, 153) to disaggregate the ear skin tissue and culture *C. auris*.

Antibiotic, antifungal treatments—To test whether antibiotic and/or antifungal receipt affected *C. auris* colonization, WT mice were pre-treated with an antibiotic cocktail [ampicillin (1 mg/ml), metronidazole (1 mg/ml), neomycin (1 mg/ml) and vancomycin (0.5 mg/ml)], fluconazole (0.25 mg/ml), or combination of antibiotics/fluconazole for four weeks. $1x10^9$ *C. auris* cells were applied onto shaved mouse dorsal skin every other day four times. Only skin topical *C. auris* levels were tested at the end of the experiment.

In a separate experiment, WT mice were treated with skin-directed antibiotics [tetracycline (0.5 mg/ml), trimethoprim/sulfamethoxazole (0.13 mg/ml trimethoprim and 0.67 mg/ml sulfamethoxazole)] for four weeks prior to colonization with $1x10^9$ *C. auris*. Skin tissue and small intestinal content were processed for culturing *C. auris*.

Diabetic, high-fat diet murine models tested—As epidemiological surveys point to diabetes as one potential clinical risk factor, we compared diabetic (db/db) mice with WT

mice. Only skin topical *C. auris* levels were tested at the end of the experiment. We further tested whether high fat diet (HFD) could promote *C. auris* skin colonization. WT mice were fed with HFD or control diet for two weeks prior to colonization. Dorsal skin was colonized, and dorsal skin tissue and intestinal content processed for culturing.

Intravenous bloodstream infection—*Candida albicans* strains SC5314 (Lionakis et al., 2013), *C. auris* East Asian clade (CDC # 0381), *C. auris* African clade (CDC # 0383), *C. auris* South American clade (CDC # 0385), *C. auris* South Asian clade (CDC # 0387) and *C. auris* NIH strain were used in the present study. Fungi were grown on YPD (Yeast extract/Peptone/Dextrose) agar plates for 48 hours to obtain single colonies. A single colony was then used to inoculate YPD broth containing penicillin/streptomycin and grown for 16-24h at 30°C. The fungal cells were centrifuged, washed once with sterile PBS and reconstituted in PBS for infections. A standard model of invasive candidiasis was utilized (Lionakis et al., 2011; Spellberg et al., 2005), where 10^5 *C. albicans* or *C. auris* blastospores were injected per mouse via lateral tail vein in 200 μl volume of PBS. Survival was monitored for 28 days.

Histological staining of mouse skin tissue—Pinnae were cut with sterile scissors and fixed in 10% formalin. After 24 hours, fixed tissue specimens were washed in 70% ethanol and sent to Histoserv (Germantown, MD) for Grocott-Gomori's methenamine silver (GMS) and Hematoxylin and Eosin (H&E) staining. For the GMS staining, ear tissue specimens were cut parallel to the ear plane to maximize the visualization of fungal cells within the ear tissue. For H&E staining, ear tissue specimens were cut perpendicular to the ear plane.

IL-22 neutralizing antibody treatment in *Act1*$^{-/-}$ mice—Three treatment groups were established, each with five female mice: *Act1*$^{-/-}$ mice injected with IL-22 neutralizing antibody, *Act1*$^{-/-}$ mice injected with isotype and WT C57BL/6NTac mice injected with isotype. Injections started one day before topical association (day −1) and lasted 15 days daily, with each mouse receiving 150 μg of antibody in a total volume of 200 μl in sterile PBS. After dorsal shaving, approximately $1x10^9$ *C. auris* cells were applied onto mouse dorsal and pinna skin every other day for four times (days 0, 2, 4, 6). Dorsal and pinna skin swabs were taken on days 4, 10 and 14. On day 14, mice were sacrificed, dorsal and ear skin tissue and intestinal content disaggregated, and CFUs from direct plating recorded.

Fluorescence activated cell sorting of immune cells isolated from disaggregated mouse ear skin tissue—Antibody staining was performed on tissue single-cell suspensions for 20-30 minutes at 4°C in Hanks' Balanced Salt Solution staining buffer and then washed twice with cold PBS. The sole exception was CD127, where staining was performed at room temperature for an hour. To measure cytokine production, cells were stimulated in vitro with Phorbol 12-myristate 13-acetate (PMA), ionomycin (Iono), and Brefeldin A (BFA) for 2 hours and 30 minutes. For intracellular staining, cells were fixed for 30 minutes with the eBioscience Fixation/Permeabilization kit as described by the manufacturer and stained intracellularly for at least 1 hour with anti-CD4, anti-CD8, anti-CD90.2, anti-TCRβ, anti-IFN-γ anti-IL-17A and anti-IL17F. Antibodies for flow cytometry were purchased from BD Biosciences, BioLegend, or eBiosciences. Antibodies used were conjugated to FITC, AF488, PE, PerCP-Cy5.5, PCP-eFluor 710, PeCy7, Alexa Fluor 780,

Pacific Blue, BV605, BV650, BV 510, BV785, eFluor 450, APC, Alexa Flour 647, PE Texas Red, PE-CF594. DAPI or Live/Dead fixable stain (Life Technologies) was used to exclude dead cells in all experiments. Flow cytometric data was acquired on an LSR II or LSR Fortessa (BD Biosciences) and analyzed using the FlowJo software (Tree Star, Version 9).

Long-term colonization by *C. auris* in *Rag2*$^{-/-}$*Il2rg*$^{-/-}$ mice—After dorsal shaving, approximately 1x10^9 *C. auris* cells were applied onto dorsal and pinna skin four times every other day of *Rag2*$^{-/-}$*Il2rg*$^{-/-}$ and matched control mice. Skin swabs and stool samples were taken during topical association, then weekly for first month, and then monthly for up to 5 months. Experiments were repeated three times, both dorsal and pinna skin were colonized for the first and third experiments, and dorsal skin was colonized for the second experiment. For these three experiments, last skin surface and stool samples were taken on day 206, 183 and 180, and skin tissue and intestinal content processed on day 232, 204 and 208, respectively.

Chlorhexidine treatment—To test its protective effect against *C. auris* colonization, 2% chlorhexidine impregnated wipes (Sage Products) were applied daily onto mouse dorsal and pinna skin for four days. After *C. auris* topical colonization, chlorhexidine was applied every other day (Figure 4A). Skin swabs were taken throughout the experiment and skin tissue processed for culturing *C. auris*.

To test the decolonizing effect of chlorhexidine against *C. auris*, experiments were performed similar to above, except chlorhexidine impregnated wipes were applied daily onto mouse dorsal and pinna skin for seven days only after topical association (Figure 4D).

Chlorhexidine retention of *C. auris* gDNA—After dorsal shaving, approximately 5x10^9/ml *C. auris* cells were applied onto mouse dorsal and pinna skin every other day for two times. Chlorhexidine was then applied every other day to the dorsal and pinna skin. On days 3, 7, 11 and 15, skin swabs were taken from the left or right ears and left or right side of the dorsal skin for CFU plating or gDNA extraction/qPCR, respectively. DNA was extracted according to established protocols (Findley et al., 2013; Jo et al., 2016). After gDNA extraction, qPCR was performed according to (Leach et al., 2018), with 2.1 μl PCR water, 0.5 μl *C. auris* qPCR primer (10 μM), 5.0 μl TaqMan Fast Advanced Master Mix, 0.4 μl *C. auris* TaqMan probe and 2.0 μl gDNA, on a QuantStudio 6 Flex platform. Two technical replicates for each mouse gDNA sample were performed.

QUANTIFICATION AND STATISTICAL ANALYSIS

Sample Sizes—N represents the number of mice as described in legends of each figure.

Statistical analysis—The Shapiro-Wilk test was first applied to test for normality. If normality was met, *t*-test or one-way analysis of variance (ANOVA) was used to prepare differences between two or more groups. If normality was not met, the non-parametric Mann-Whitney U test or Kruskal–Wallis one-way ANOVA was used to prepare differences between two or more groups. For parametric ANOVA tests, the Tukey's honestly significant difference (HSD) test was used for comparing differences between two groups post ANOVA

with equal variances, and the Games-Howell post-hoc test used with unequal variances. For non-parametric ANOVA tests, the Dunn's test was used to compare between two groups post hoc. Statistical analyses were performed using R (v3.6.0) and Prism (v8).

Supplementary Material

Refer to Web version on PubMed Central for supplementary material.

Acknowledgments

Research was funded by the Division of Intramural Research of the NHGRI and NIAID, NIH. The authors would like to thank Qiong Chen, ShihQueen Lee-Lin and Michael Abers for technical assistance with experiments, as well as Stephen Wincovitch for digitalization and visualization of histological slides. Darryl Leja crafted the Graphical Abstract. Helpful discussions and comments on the manuscript were provided by Ana Litvintseva, Tara Palmore, Heidi Kong and members of the Segre and Lionakis labs.

References

Adams E, Quinn M, Tsay S, Poirot E, Chaturvedi S, Southwick K, Greenko J, Fernandez R, Kallen A, Vallabhaneni S, et al. (2018). *Candida auris* in Healthcare Facilities, New York, USA, 2013-2017. Emerg Infect Dis. 24(10), 1816–1824. [PubMed: 30226155]

Ben-Ami R, Berman J, Novikov A, Bash E, Shachor-Meyouhas Y, Zakin S, Maor Y, Tarabia J, Schechner V, Adler A, et al. (2017). Multidrug-Resistant *Candida haemulonii* and *C. auris*, Tel Aviv, Israel. Emerg Infect Dis. 23(1).

Bishu S, Hernández-Santos N, Simpson-Abelson MR, Huppler AR, Conti HR, Ghilardi N, Mamo AJ and Gaffen SL (2014). The adaptor CARD9 is required for adaptive but not innate immunity to oral mucosal *Candida albicans* infections. Infect. Immun. 82(3), 1173–1180. [PubMed: 24379290]

Boisson B, Wang C, Pedergnana V, Wu L, Cypowyj S, Rybojad M, Belkadi A, Picard C, Abel L, Fieschi C, et al. (2013). An ACT1 mutation selectively abolishes interleukin-17 responses in humans with chronic mucocutaneous candidiasis. Immunity. 39(4), 676–686. [PubMed: 24120361]

Cassir N, Papazian L, Fournier PE, Raoult D, and La Scola B (2015). Insights into bacterial colonization of intensive care patients' skin: the effect of chlorhexidine daily bathing. Eur J Clin Microbiol. 34(5), 999–1004.

Centers for Disease Control and Prevention (CDC). Antibiotic Resistance Threats in the United States, 2019 Atlanta: CDC https://www.cdc.gov/drugresistance/pdf/threats-report/2019-arthreats-report-508.pdf.

Chow NA, de Groot T, Badali H, Abastabar M, Chiller TM, and Meis JF (2019). Potential Fifth Clade of *Candida auris*, Iran, 2018. Emerging Infectious Diseases. 25(9), 1780–1781. [PubMed: 31310230]

Chow NA, Gade L, Tsay SV, Forsberg K, Greenko JA, Southwick KL, Barrett PM, Kerins JL, Lockhart SR, Chiller TM, et al. (2018). Multiple introductions and subsequent transmission of multidrug-resistant *Candida auris* in the USA: a molecular epidemiological survey. Lancet Infect Dis. 18(12), 1377–1384. [PubMed: 30293877]

Chow NA, Muñoz JF, Gade L, Berkow E, Li X, Welsh RM, Forsberg K, Lockhart SR, Adam R, Alanio A, et al. (2020). Tracing the evolutionary history and global expansion of *Candida auris* using population genomic analyses. bioRxiv. 2020.2001.2006.896548.

Conti HR, Bruno VM, Childs EE, Daugherty S, Hunter JP, Mengesha BG, Saevig DL, Hendricks MR, Coleman BM, Brane L, et al. (2016). IL-17 Receptor Signaling in Oral Epithelial Cells Is Critical for Protection against Oropharyngeal Candidiasis. Cell Host Microbe. 20(5), 606–617. [PubMed: 27923704]

Eyre DW, Sheppard AE, Madder H, Moir I, Moroney R, Quan TP, Griffiths D, George S, Butcher L, Morgan M, et al. (2018). A *Candida auris* Outbreak and Its Control in an Intensive Care Setting. N Engl J Med. 379(14), 1322–1331. [PubMed: 30281988]

Fakhim H, Vaezi A, Dannaoui E, Chowdhary A, Nasiry D, Faeli L, Meis JF, and Badali H (2018). Comparative virulence of *Candida auris* with *Candida haemulonii*, *Candida glabrata* and *Candida albicans* in a murine model. Mycoses. 61(6), 377–382. [PubMed: 29460345]

Findley K, Oh J, Yang J, Conlan S, Deming C, Meyer JA, Schoenfeld D, Nomicos E, Park M, Program NIHISCCS, et al. (2013). Topographic diversity of fungal and bacterial communities in human skin. Nature. 498(7454), 367–370. [PubMed: 23698366]

Forsberg K, Woodworth K, Walters M, Berkow EL, Jackson B, Chiller T, and Vallabhaneni S (2019). *Candida auris*: The recent emergence of a multidrug-resistant fungal pathogen. Med Mycol. 57(1), 1–12. [PubMed: 30085270]

Frieder J, Kivelevitch D, Haugh I, Watson I, and Menter A (2018). Anti-IL-23 and Anti-IL-17 Biologic Agents for the T reatment of Immune-Mediated Inflammatory Conditions. Clin Pharmacol Ther. 103(1), 88–101. [PubMed: 28960267]

Grice EA, Snitkin ES, Yockey LJ, Bermudez DM, Program NCS, Liechty KW, and Segre JA (2010). Longitudinal shift in diabetic wound microbiota correlates with prolonged skin defense response. Proc Natl Acad Sci U S A. 107(33), 14799–14804. [PubMed: 20668241]

Guggino G, Giardina A, Ferrante A, Giardina G, Schinocca C, Sireci G, Dieli F, Ciccia F, and Triolo G (2015). The in vitro addition of methotrexate and/or methylprednisolone determines peripheral reduction in Th17 and expansion of conventional Treg and of IL-10 producing Th17 lymphocytes in patients with early rheumatoid arthritis. Rheumatol Int. 35(1), 171–175. [PubMed: 24792332]

Harrison OJ, Linehan JL, Shih HY, Bouladoux N, Han SJ, Smelkinson M, Sen SK, Byrd AL, Enamorado M, Yao C, et al. (2019). Commensal-specific T cell plasticity promotes rapid tissue adaptation to injury. Science. 363(6422), eaat6280. [PubMed: 30523076]

Huang SS, Septimus E, Kleinman K, Moody J, Hickok J, Avery TR, Lankiewicz J, Gombosev A, Terpstra L, Hartford F, et al. (2013). Targeted versus universal decolonization to prevent ICU infection. N Engl J Med. 368(24), 2255–2265. [PubMed: 23718152]

Huang SS, Septimus E, Kleinman K, Moody J, Hickok J, Heim L, Gombosev A, Avery TR, Haffenreffer K, Shimelman L, et al. (2019a). Chlorhexidine versus routine bathing to prevent multidrug-resistant organisms and all-cause bloodstream infections in general medical and surgical units (ABATE Infection trial): a cluster-randomised trial. Lancet. 393(10177), 1205–1215. [PubMed: 30850112]

Huang SS, Singh R, McKinnell JA, Park S, Gombosev A, Eells SJ, Gillen DL, Kim D, Rashid S, Macias-Gil R, et al. (2019b). Decolonization to Reduce Postdischarge Infection Risk among MRSA Carriers. New Engl J Med. 380(7), 638–650. [PubMed: 30763195]

Igyarto BZ, Haley K, Ortner D, Bobr A, Gerami-Nejad M, Edelson BT, Zurawski SM, Malissen B, Zurawski G, Berman J, et al. (2011). Skin-resident murine dendritic cell subsets promote distinct and opposing antigen-specific T helper cell responses. Immunity. 35(2), 260–272. [PubMed: 21782478]

Jackson BR, Chow N, Forsberg K, Litvintseva AP, Lockhart SR, Welsh R, Vallabhaneni S, and Chiller T (2019). On the Origins of a Species: What Might Explain the Rise of *Candida auris*? J Fungi. 5(3).

Jo JH, Deming C, Kennedy EA, Conlan S, Polley EC, Ng WI, Program NCS, Segre JA, and Kong HH (2016). Diverse Human Skin Fungal Communities in Children Converge in Adulthood. J Invest Dermatol. 136(12), 2356–2363. [PubMed: 27476723]

Kampf G (2016). Acquired resistance to chlorhexidine - is it time to establish an 'antiseptic stewardship' initiative? J Hosp Infect. 94(3), 213–227. [PubMed: 27671220]

Kashem SW, Igyarto BZ, Gerami-Nejad M, Kumamoto Y, Mohammed JA, Jarrett E, Drummond RA, Zurawski SM, Zurawski G, Berman J, et al. (2015). *Candida albicans* morphology and dendritic cell subsets determine T helper cell differentiation. Immunity. 42(2), 356–366. [PubMed: 25680275]

Kashem SW, and Kaplan DH (2016). Skin immunity to *Candida albicans*. Trends Immunol. 37(7), 440–450. [PubMed: 27178391]

Kashem SW, Riedl MS, Yao C, Honda CN, Vulchanova L and Kaplan DH (2015). Nociceptive sensory fibers drive interleukin-23 production from CD301b+ dermal dendritic cells and drive protective cutaneous immunity. Immunity. 43(3), 515–526. [PubMed: 26377898]

Kates AE, Zimbric ML, Mitchell K, Skarlupka J, and Safdar N (2019). The impact of chlorhexidine gluconate on the skin microbiota of children and adults: A pilot study. Am J Infect Control. 47(8), 1014–1016. [PubMed: 30879799]

Khan Z, Ahmad S, Benwan K, Purohit P, Al-Obaid I, Bafna R, Emara M, Mokaddas E, Abdullah AA, Al-Obaid K, et al. (2018). Invasive *Candida auris* infections in Kuwait hospitals: epidemiology, antifungal treatment and outcome. Infection. 46(5), 641–650. [PubMed: 29949089]

Kobayashi T, Glatz M, Horiuchi K, Kawasaki H, Akiyama H, Kaplan DH, Kong HH, Amagai M, and Nagao K (2015). Dysbiosis and *Staphylococcus aureus* Colonization Drives Inflammation in Atopic Dermatitis. Immunity. 42(4), 756–766. [PubMed: 25902485]

Kordalewska M, Zhao Y, Lockhart SR, Chowdhary A, Berrio I, and Perlin DS (2017). Rapid and Accurate Molecular Identification of the Emerging Multidrug-Resistant Pathogen *Candida auris*. J Clin Microbiol. 55(8), 2445–2452. [PubMed: 28539346]

Larkin E, Hager C, Chandra J, Mukherjee PK, Retuerto M, Salem I, Long L, Isham N, Kovanda L, Borroto-Esoda K, et al. (2017). The Emerging Pathogen *Candida auris*: Growth Phenotype, Virulence Factors, Activity of Antifungals, and Effect of SCY-078, a Novel Glucan Synthesis Inhibitor, on Growth Morphology and Biofilm Formation. Antimicrobial Agents and Chemotherapy. 61(5).

Leach L, Zhu Y, and Chaturvedi S (2018). Development and Validation of a Real-Time PCR Assay for Rapid Detection of Candida auris from Surveillance Samples. J Clin Microbiol. 56(2).

LeibundGut-Landmann S, Gross O, Robinson MJ, Osorio F, Slack EC, Tsoni SV, Schweighoffer E, Tybulewicz V, Brown GD, Ruland J, et al. (2007). Syk- and CARD9-dependent coupling of innate immunity to the induction of T helper cells that produce interleukin 17. Nat Immunol. 8(6), 630–638. [PubMed: 17450144]

Lionakis MS, and Hohl TM (2020). Call to Action: How to Tackle Emerging Nosocomial Fungal Infections. Cell Host Microbe. 27(6), 859–862. [PubMed: 32526182]

Lionakis MS, and Levitz SM (2018). Host Control of Fungal Infections: Lessons from Basic Studies and Human Cohorts. Annu Rev Immunol. 36, 157–191. [PubMed: 29237128]

Lionakis MS, Lim JK, Lee CC, and Murphy PM (2011). Organ-specific innate immune responses in a mouse model of invasive candidiasis. J Innate Immun. 3(2), 180–199. [PubMed: 21063074]

Lionakis MS, and Netea MG (2013). *Candida* and host determinants of susceptibility to invasive candidiasis. Plos Pathog. 9(1), e1003079. [PubMed: 23300452]

Lionakis MS, Swamydas M, Fischer BG, Plantinga TS, Johnson MD, Jaeger M, Green NM, Masedunskas A, Weigert R, Mikelis C, et al. (2013). CX3CR1-dependent renal macrophage survival promotes Candida control and host survival. J Clin Invest. 123(12), 5035–5051. [PubMed: 24177428]

Lockhart SR, Etienne KA, Vallabhaneni S, Farooqi J, Chowdhary A, Govender NP, Colombo AL, Calvo B, Cuomo CA, Desjardins CA, et al. (2017). Simultaneous Emergence of Multidrug-Resistant *Candida auris* on 3 Continents Confirmed by Whole-Genome Sequencing and Epidemiological Analyses. Clin Infect Dis. 64(2), 134–140. [PubMed: 27988485]

Marakalala MJ, Vautier S, Potrykus J, Walker LA, Shepardson KM, Hopke A, Mora-Montes HM, Kerrigan A, Netea MG, Murray GI, et al. (2013). Differential adaptation of *Candida albicans* in vivo modulates immune recognition by dectin-1. Plos Pathog. 9(4), e1003315. [PubMed: 23637604]

Naik S, Bouladoux N, Linehan JL, Han SJ, Harrison OJ, Wilhelm C, Conlan S, Himmelfarb S, Byrd AL, Deming C, et al. (2015). Commensal-dendritic-cell interaction specifies a unique protective skin immune signature. Nature. 520(7545), 104–108. [PubMed: 25539086]

Naik S, Bouladoux N, Wilhelm C, Molloy MJ, Salcedo R, Kastenmuller W, Deming C, Quinones M, Koo L, Conlan S, et al. (2012). Compartmentalized control of skin immunity by resident commensals. Science. 337(6098), 1115–1119. [PubMed: 22837383]

Ostrowsky B, Greenko J, Adams E, Quinn M, O'Brien B, Chaturvedi V, Berkow E, Vallabhaneni S, Forsberg K, Chaturvedi S, et al. (2020). *Candida auris* Isolates Resistant to Three Classes of Antifungal Medications - New York, 2019. MMWR Morb Mortal Wkly Rep. 69(1), 6–9. [PubMed: 31917780]

Pappas PG, Lionakis MS, Arendrup MC, Ostrosky-Zeichner L, and Kullberg BJ (2018). Invasive candidiasis. Nat Rev Dis Primers. 4, 18026. [PubMed: 29749387]

Parra-Giraldo CM, Valderrama SL, Cortes-Fraile G, Garzon JR, Ariza BE, Morio F, Linares-Linares MY, Ceballos-Garzon A, de la Hoz A, Hernandez C, et al. (2018). First report of sporadic cases of *Candida auris* in Colombia. Int J Infect Dis. 69, 63–67. [PubMed: 29421668]

Puel A, Cypowyj S, Bustamante J, Wright JF, Liu L, Lim HK, Migaud M, Israel L, Chrabieh M, Audry M, et al. (2011). Chronic mucocutaneous candidiasis in humans with inborn errors of interleukin-17 immunity. Science. 332(6025), 65–68. [PubMed: 21350122]

Ridaura VK, Bouladoux N, Claesen J, Chen YE, Byrd AL, Constantinides MG, Merrill ED, Tamoutounour S, Fischbach MA, and Belkaid Y (2018). Contextual control of skin immunity and inflammation by *Corynebacterium*. J Exp Med. 215(3), 785–799. [PubMed: 29382696]

Ruiz-Gaitan A, Moret AM, Tasias-Pitarch M, Aleixandre-Lopez AI, Martinez-Morel H, Calabuig E, Salavert-Lleti M, Ramirez P, Lopez-Hontangas JL, Hagen F, et al. (2018). An outbreak due to *Candida auris* with prolonged colonisation and candidaemia in a tertiary care European hospital. Mycoses. 61(7), 498–505. [PubMed: 29655180]

Rutala WA, Kanamori H, Gergen MF, Sickbert-Bennett EE, and Weber DJ (2019). Susceptibility of *Candida auris* and *Candida albicans* to 21 germicides used in healthcare facilities. Infect Cont Hosp Ep. 40(3), 380–382.

SanMiguel AJ, Meisel JS, Horwinski J, Zheng Q, Bradley CW, and Grice EA (2018). Antiseptic Agents Elicit Short-Term, Personalized, and Body Site-Specific Shifts in Resident Skin Bacterial Communities. J Invest Dermatol. 138(10), 2234–2243. [PubMed: 29753031]

Satoh K, Makimura K, Hasumi Y, Nishiyama Y, Uchida K, and Yamaguchi H (2009). *Candida auris sp. nov.*, a novel ascomycetous yeast isolated from the external ear canal of an inpatient in a Japanese hospital. Microbiol Immunol. 53(1), 41–44. [PubMed: 19161556]

Saunte DM, Mrowietz U, Puig L, and Zachariae C (2017). *Candida* infections in patients with psoriasis and psoriatic arthritis treated with interleukin-17 inhibitors and their practical management. Brit J Dermatol. 177(1), 47–62. [PubMed: 27580411]

Schelenz S, Hagen F, Rhodes JL, Abdolrasouli A, Chowdhary A, Hall A, Ryan L, Shackleton J, Trimlett R, Meis JF, et al. (2016). First hospital outbreak of the globally emerging *Candida auris* in a European hospital. Antimicrob Resist Infect Control. 5, 35. [PubMed: 27777756]

Septimus EJ, and Schweizer ML (2016). Decolonization in Prevention of Health Care-Associated Infections. Clin Microbiol Rev. 29(2), 201–222. [PubMed: 26817630]

Singh S, Uppuluri P, Mamouei Z, Alqarihi A, Elhassan H, French S, Lockhart SR, Chiller T, Edwards JE, and Ibrahim AS (2019). The NDV-3A vaccine protects mice from multidrug resistant *Candida auris* infection. Plos Pathog. 15(8).

Sonder SU, Saret S, Tang W, Sturdevant DE, Porcella SF, and Siebenlist U (2011). IL-17-induced NF-kappaB activation via CIKS/Act1: physiologic significance and signaling mechanisms. J Biol Chem. 286(15), 12881–12890. [PubMed: 21335551]

Sparber F, De Gregorio C, Steckholzer S, Ferreira FM, Dolowschiak T, Ruchti F, Kirchner FR, Mertens S, Prinz I, Joller N, et al. (2019). The skin commensal yeast *Malassezia* triggers a type 17 response that coordinates anti-fungal immunity and exacerbates skin inflammation. Cell Host Microbe. 25(3), 389–403. [PubMed: 30870621]

Spellberg B, Ibrahim AS, Edwards JE Jr., and Filler SG (2005). Mice with disseminated candidiasis die of progressive sepsis. J Infect Dis. 192(2), 336–343. [PubMed: 15962230]

Torres SR, Pichowicz A, Torres-Velez F, Song R, Singh N, Lasek-Nesselquist E, and De Jesus M (2019). Impact of *Candida auris* infection in a neutropenic murine model. Antimicrobial Agents and Chemotherapy. AAC.01625–01619.

Vallabhaneni S, Jackson BR, and Chiller TM (2019). *Candida auris*: An Emerging Antimicrobial Resistance Threat. Ann Intern Med. 171(6), 432–433. [PubMed: 31357215]

Vallabhaneni S, Kallen A, Tsay S, Chow N, Welsh R, Kerins J, Kemble SK, Pacilli M, Black SR, Landon E, et al. (2016). Investigation of the First Seven Reported Cases of *Candida auris*, a Globally Emerging Invasive, Multidrug-Resistant Fungus - United States, May 2013-August 2016. MMWR Morb Mortal Wkly Rep. 65(44), 1234–1237. [PubMed: 27832049]

Wang X, Bing J, Zheng Q, Zhang F, Liu J, Yue H, Tao L, Du H, Wang Y, Wang H, et al. (2018). The first isolate of *Candida auris* in China: clinical and biological aspects. Emerg Microbes Infect. 7(1), 93. [PubMed: 29777096]

Welsh RM, Bentz ML, Shams A, Houston H, Lyons A, Rose LJ, and Litvintseva AP (2017). Survival, Persistence, and Isolation of the Emerging Multidrug-Resistant Pathogenic Yeast *Candida auris* on a Plastic Health Care Surface. J Clin Microbiol. 55(10), 2996–3005. [PubMed: 28747370]

Wurster S, Bandi A, Beyda ND, Albert ND, Raman NM, Raad II, and Kontoyiannis DP (2019). Drosophila melanogaster as a model to study virulence and azole treatment of the emerging pathogen *Candida auris*. J Antimicrob Chemoth. 74(7), 1904–1910.

Xin H, Mohiuddin F, Tran J, Adams A, and Eberle K (2019). Experimental Mouse Models of Disseminated *Candida auris* Infection. Msphere. 4(5).

Zhu Y, O'Brien B, Leach L, Clark A, Bates M, Adams E, Ostrowsky B, Quinn M, Dufort E, Southwick K, et al. (2019). Laboratory Analysis of an Outbreak of *Candida auris* in New York from 2016 to 2018-Impact and Lessons Learned. J Clin Microbiol. 58(4), e01503–01519.

Highlights

- Fungal pathogen *Candida auris* colonizes mouse skin surface and tissue.
- *C. auris* clades, of distinct geographic regions, differentially colonize mouse skin.
- IL-17 receptor signaling protects mice from long-term *C. auris* colonization.
- Chlorhexidine antiseptic protects against colonization of *C. auris* on mouse skin.

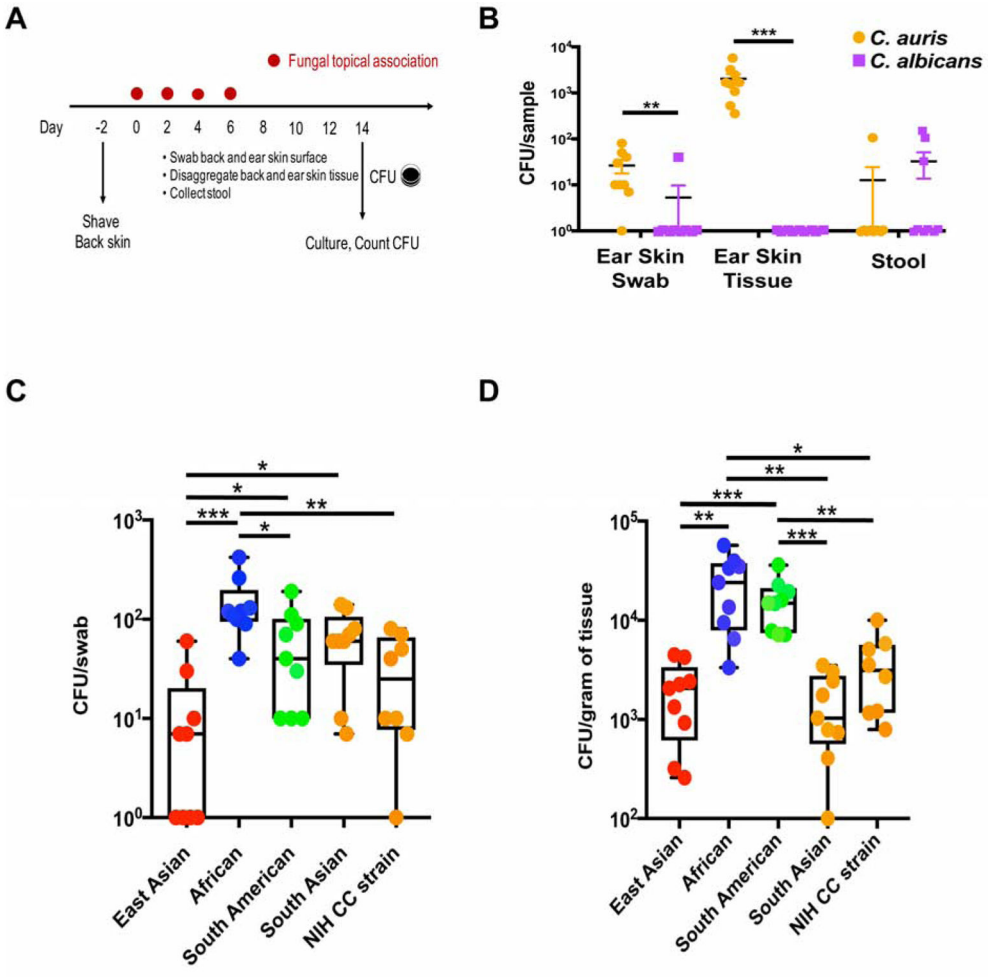

Figure 1. *Candida auris* colonizes skin surface and tissue compartment with clade specificity.

(A) Schematic for experimental design. Fungal cells were topically associated on ear pinna and dorsal back skin every other day four times. Skin swabs, skin tissue and stool were obtained on day 14 and processed for *C. auris* culturing.

(B) *C. auris* colonizes skin surface and tissue but not the gut compartment. Colony forming units (CFUs) per swab, gram of tissue or gram of stool from wild-type (WT) mice colonized with *C. auris* (orange) and *C. albicans* (purple) are plotted. Shown are mean values +/− SEM. Statistics were calculated using the Mann-Whitney U test. N=9 mice for each group, two independent experiments. See also Figure S1A and Table S1.

(C and D) *C. auris* colonization of WT mice with each of the four clades or the NIH Clinical Center strain (South Asian clade) was measured by culturing skin swabs (C) and disaggregated skin tissue (D). Statistics were calculated using one-way ANOVA with Tukey's post-hoc tests or Games-Howell tests, as appropriate. N=8-9 mice for each group, two independent experiments. See also Figure S2.

*: $p<0.05$, **: $p<0.01$, ***: $p<0.001$.

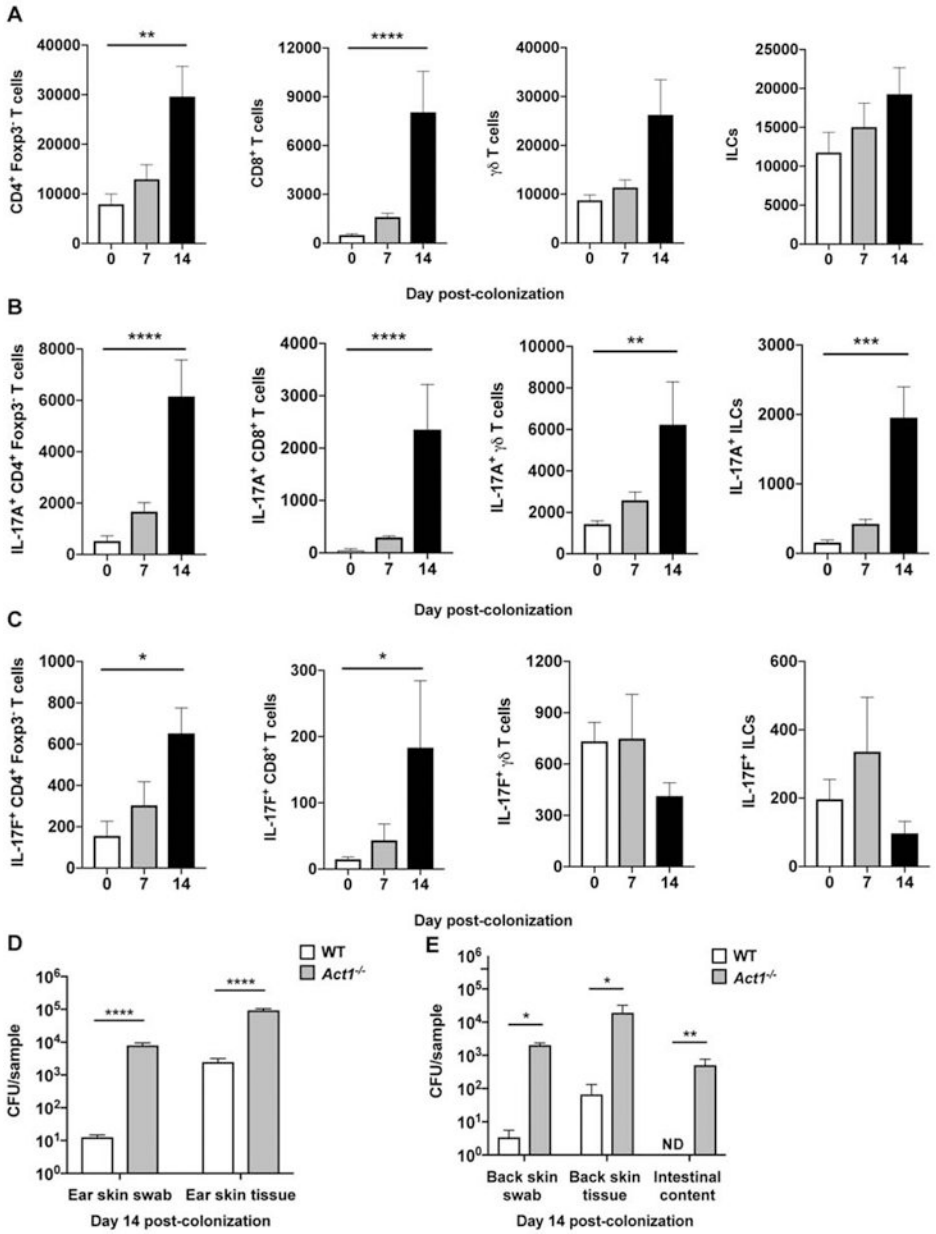

Figure 2. *C. auris* elicits a protective IL-17A/IL-17F response derived from innate and adaptive lymphoid cells.

(A) Accumulation of $CD4^+$ T cells, $CD8^+$ T cells, γδ T cells, and innate lymphoid cells (ILCs) in the skin of WT mice 7 and 14 days after *C. auris* topical association as compared with naïve WT mice.

(B-C) Differences in IL-17A-producing (A) and IL-17F-producing (B) $CD4^+$ T cells, $CD8^+$ T cells, γδ T cells, and ILCs are shown for naïve WT mice, and WT mice 7 and 14 days after topical association with *C. auris*. (A-C) Total number of cells are shown for each cell type. Statistics were calculated using one-way ANOVA with Tukey's HSD post-hoc test or Kruskal-Wallis test with Dunn's multiple comparison test, as appropriate. N=6-9 mice for

each group; two independent experiments. Data are shown with mean ± SEM. See also Figures S3, S4A-C and S5.

(D) Mice deficient in *Act1*, an essential adaptor of IL-17R family signaling, are defective in clearing *C. auris* from the ear skin surface (CFU/swab) and ear skin tissue (CFU/gram of tissue) relative to WT mice, measured 14 days after *C. auris* topical association. Statistics were calculated using the Mann-Whitney U test. N=10 mice for each group; two independent experiments. Data are shown with mean ± SEM.

(E) Compared with WT, mice deficient in *Act1* have increased *C. auris* on the back skin surface (CFU/swab), back skin tissue (CFU/gram of tissue) and intestinal compartments (CFU/gram of intestinal content) on day 14 after topical *C. auris* association. Statistics were calculated using the Mann-Whitney U test. N=4-5 mice for each group. Data are shown with mean ± SEM.

*: $p<0.05$, **: $p<0.01$, ***: $p<0.001$, ****: $p<0.0001$, ND: not detected.

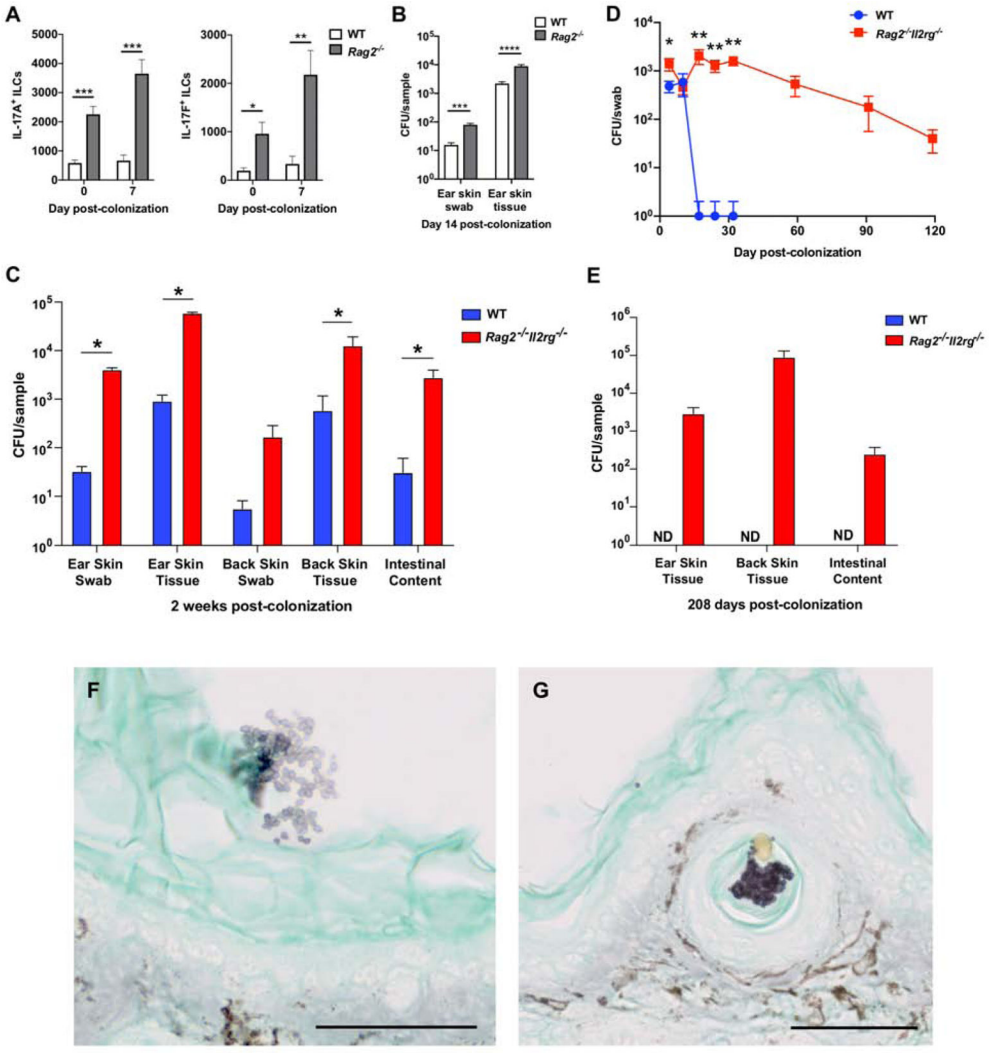

Figure 3. Immunodeficient *Rag2*$^{-/-}$ and *Rag2*$^{-/-}$*Il2rg*$^{-/-}$ mice exhibit greater propensity for *C. auris* skin colonization.

(A) IL-17A and IL-17F production by ILCs is increased in the skin of *Rag2*$^{-/-}$ mice. Shown are numbers of IL-17A-producing (left panel) and IL-17F-producing (right panel) ILCs in the skin of WT and Rag2-deficient mice at steady state and 7 days after *C. auris* colonization. The statistics were calculated using the *t*-test or Mann-Whitney U test, as appropriate. N=6-9 mice for each group; two independent experiments. Data are mean ± SEM.

(B) *Rag2*$^{-/-}$ mice are defective in controlling *C. auris* colonization on the ear skin surface (CFU/swab) and within the tissue compartment (CFU/gram of tissue). The statistics were calculated using the *t*-test or Mann-Whitney U test, as appropriate. N=9-10 mice for each group; two independent experiments.

(C) Immunodeficient *Rag2*$^{-/-}$*Il2rg*$^{-/-}$ mice are defective in clearing *C. auris* from the ear and back skin surface (CFU/swab) and tissue (CFU/gram of tissue); and intestinal compartments (CFU/gram of intestinal content) as determined by culturing from WT and *Rag2*$^{-/-}$*Il2rg*$^{-/-}$ mice two weeks after topical colonization. The statistics were calculated

using the Mann-Whitney U test. N=5 mice for each group, representative of two independent experiments. Data are shown with mean ± SEM. See also Figure S4G-H.

(D) Longitudinally, WT and *Rag2*$^{-/-}$*Il2rg*$^{-/-}$ mouse skin swabs were cultured for *C. auris* on days 4, 10, 17, 24, 32, and extended through days 59, 91 and 119 for *Rag2*$^{-/-}$*Il2rg*$^{-/-}$ mice. The Mann-Whitney U test was used to compare between WT and *Rag2*$^{-/-}$*Il2rg*$^{-/-}$ mice at each time point up to day 32. N=6 mice for each group, representative of three independent experiments. Data are shown with mean ± SEM.

(E) Immunodeficient *Rag2*$^{-/-}$*Il2rg*$^{-/-}$ mice are defective in clearing *C. auris* from the ear and back skin tissue (CFU/gram of tissue); and intestinal compartments (CFU/gram of intestinal content) as measured by culturing from WT and *Rag2*$^{-/-}$*Il2rg*$^{-/-}$ mice 208 days after topical association. No *C. auris* colonies were cultured from WT mice on day 208. N=6 mice for each group, representative of three independent experiments. Data are shown with mean ± SEM. ND: not detected.

(F and G) Grocott-Gomori's methenamine silver stain for fungi from ear pinna sections of a *Rag2*$^{-/-}$*Il2rg*$^{-/-}$ mouse colonized by *C. auris* 7 days after topical association. Clusters of *C. auris* cells (purple) can be seen on the skin surface (stratum corneum, F) and located inside a hair follicle (G). 50 μm scale bar is displayed at the bottom right. The brown stain is endogenous mouse skin pigment also observed on control uncolonized mice. See also Figure S1A.

*: $p<0.05$, **: $p<0.01$, ***: $p<0.001$, ****: $p<0.0001$.

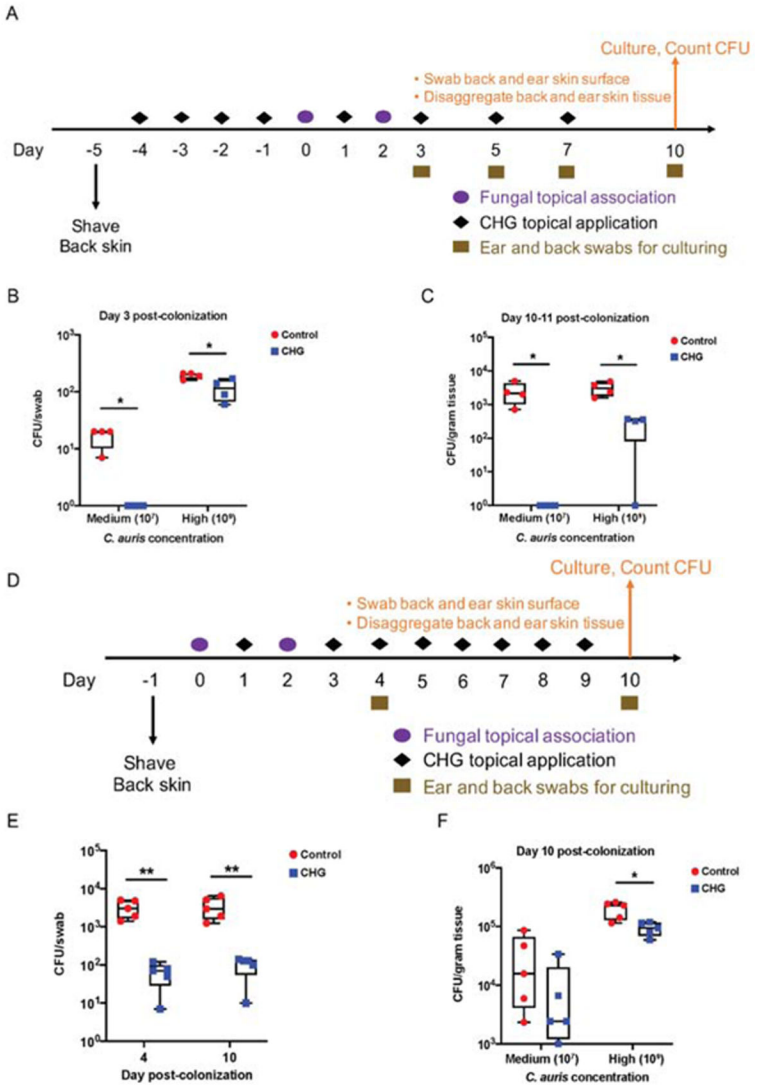

Figure 4. Skin antiseptic chlorhexidine protects WT mice from *C. auris* colonization and promotes *C. auris* decolonization of *Rag2*$^{-/-}$*Il2rg*$^{-/-}$ mice.

(A) Schematic for experimental design to model chlorhexidine gluconate (CHG) skin bathing. Wipes impregnated with CHG were used daily for four days to 'bathe' the mouse skin before topical association. Cotton gauze saturated with sterile PBS was used as procedural control. *C. auris* cells were topically associated onto mouse ear pinna and dorsal back skin at two concentrations: 10^7 CFU as medium concentration, and 10^9 CFU as high concentration. After topical association, CHG was applied every other day for the duration of the experiment. Skin swabs were taken during the experiment and skin tissues were disaggregated at the end of the experiment and processed for *C. auris* culturing.

(B) CHG bathing protects WT mouse skin from *C. auris* topical exposure (medium and high concentrations) as measured by culturing skin swabs. N=4 mice for each group, representative of two independent experiments.

(C) CHG bathing protects WT mouse skin tissue from *C. auris* residence after topical exposure (medium and high concentrations). N=4 mice for each group, representative of two independent experiments.
(D) Schematic for experimental design to model CHG skin bathing to promote *C. auris* decolonization. After *C. auris* (medium and high concentrations) topical association, daily bathing with CHG was deployed for one week. Skin swabs were taken during the experiment and skin tissues were disaggregated at the end of the experiment for culturing.
(E) CHG bathing promotes *C. auris* decolonization on *Rag2*$^{-/-}$*Il2rg*$^{-/-}$ ear skin swabs 4 and 10 days after high concentration topical exposure. The statistics were calculated using the *t*-test. N=5 mice for each group, representative of two independent experiments.
(F) CHG bathing promotes *C. auris* decolonization in *Rag2*$^{-/-}$*Il2rg*$^{-/-}$ resident skin tissue after medium and high concentration topical exposure. N=5 mice for each group, representative of two independent experiments. See also Table S3. (B,C,E,F) The statistics were calculated using the *t*-test.
*: $p<0.05$, **: $p<0.01$.

KEY RESOURCES TABLE

REAGENT or RESOURCE	SOURCE	IDENTIFIER
Antibodies		
Anti-mouse B220, PE-CF594 (RA3-6B2)	BD Biosciences	Cat # 562290
Anti-mouse CCR6, PE (29-2L17)	Biolegend	Cat # 129804
Anti-mouse CD4, AF700 (RM4-5)	eBioscience	Cat # 56-0042-82
Anti-mouse CD4, BV510 (RM4-5)	BD Biosciences	Cat # 563106
Anti-Mouse CD5, BV510	Biolegend	Cat # 100627
Anti-mouse CD8β, BV605 (H35-17.2)	BD Biosciences	Cat # 740387
Anti-mouse CD8β, BV650 (H35-17.2)	eBioscience	Cat # 740552
Anti-mouse CD8β, BUV395 (H35-17.2)	BD Biosciences	Cat #740278
Anti-mouse CD11b, BV785 (M1/70)	Biolegend	Cat # 101243
Anti-mouse CD11c, APC-eFluor 780 (N418)	eBioscience	Cat # 47-0114-82
Anti-mouse CD44, AF700 (IM7)	eBioscience	Cat # 56-0441-82
Anti-mouse CD44, PeCy7 (IM7)	eBioscience	Cat # 25-0441-82
Anti-mouse CD45, APC-eFluor 780 (30-F11)	eBioscience	Cat # 47-0451-82
Anti-mouse CD45, BV510 (30-F11)	Biolegend	Cat # 103138
Anti-mouse CD90.2, BV605 (53-2.1)	Biolegend	Cat # 140318
Anti-mouse CD90.2, BV785 (30-H12)	Biolegend	Cat # 105331
Anti-mouse CD103, PerCP-eFluor 710 (2E7)	eBioscience	Cat # 46-1031-82
anti-mouse CD127 (IL-7Rα), BV605	Biolegend	Cat # 135041
Anti-mouse FoxP3, APC (FJK-16s)	eBioscience	Cat #17-5773-82
Anti-mouse FoxP3, FITC (FJK-16s)	eBioscience	Cat # 11-5773-82
Anti-mouse Ly-6C, BV605 (HK1.4)	Biolegend	Cat # 128036
Anti-mouse Ly-6G, PE-Cy7 (1A8)	BD Biosciences	Cat # 560601
Anti-mouse MHC-II, AF700 (M5/114.15.2)	eBioscience	Cat # 56-5321-82
Anti-mouse NK1.1, PE-CF594 (PK136)	BD Biosciences	Cat # 562864
Anti-mouse RORγt, PE-CF594 (Q31-378)	BD Biosciences	Cat #562684
Anti-mouse TCRβ, PerCP-Cy5.5 (H57-597)	eBioscience	Cat # 45-5961-82
Anti-mouse TCRβ, BUV737 (H57-597)	BD Biosciences	Cat # 612821
Anti-mouse TCRγδ, BV650 (GL3)	BD Biosciences	Cat # 563993
Anti-mouse TCRγδ, PE-CF594 (GL3)	BD Biosciences	Cat # 563532
Anti-mouse IFN-γ, eFluor450 (XMG1.2)	eBioscience	Cat # 48-7311-82
Anti-mouse IFN-γ, Brilliant Violet 605 (XMG1.2)	Biolegend	Cat #505840
Anti-mouse IL-5, APC	Biolegend	Cat # 504304
Anti-mouse IL-13, PerCP-EF710 (eBio13A)	eBioscience	Cat # 46-7133-82
Anti-mouse IL-17A, Pe-Cy7 (TC11-18H10.1)	Biolegend	Cat # 506922
Anti-mouse IL-17F, PE (9D3.1C8)	Biolegend	Cat #517008
IL-22 neutralizing antibody	Genentech (under a material transfer agreement)	Clone 8E11

REAGENT or RESOURCE	SOURCE	IDENTIFIER
Mouse IgG1 isotype control	Bio X Cell	Clone MOPC-21 Cat # BE0083
Fungal Strains		
Candida auris, East Asia	CDC	0381
Candida auris, Africa	CDC	0383
Candida auris, South America	CDC	0385
Candida auris, South Asia	CDC	0387
Candida auris, NIH Clinical Center	NIH	N/A
Candida albicans, SC5314	ATCC	Cat # ATCC MYA-2876
Chemicals, Peptides, and Recombinant Proteins		
0.5 M EDTA pH 8	Corning	Cat # MT-46034CI
Round-Bottom Polypropylene Tubes	Corning	Cat # 352059
Ampicillin	NIH Veterinary Pharmacy	N/A
Metronidazole	NIH Veterinary Pharmacy	N/A
Neomycin	NIH Veterinary Pharmacy	N/A
Vancomycin	NIH Veterinary Pharmacy	N/A
Tetracycline	NIH Veterinary Pharmacy	N/A
Trimethoprim-Sulfamethoxazole	NIH Veterinary Pharmacy	N/A
BD Liquid Amies Elution Swab (Eswab) Collection/Transport System (BD 220245)	Fisher Scientific	Cat # 22-349-700
Chloramphenicol	Sigma	Cat # C0378-5G
BD BBL™ Prepared Plated Media: CHROMagar™ Candida (BD 254093)	Fisher Scientific	Cat # B4354093
Brefeldin A (GolgiPlug)	BD Biosciences	Cat #555029
Collagenase D	Sigma Aldrich	Cat # 11088866001
Control diet	Envigo	Cat # TD.08806
Deoxyribonuclease I from bovine pancreas	Sigma Aldrich	Cat # DN25-5G
Ethyl Alcohol 200 Proof	Pharmco-Aaper	Cat # 111000200
Fetal bovine serum	HyClone	Cat # C838R85
Filcon, Sterile, Syringe-Type, 50 μm	BD Bioscience	Cat # 340601
Fluconazole, ≥98% (HPLC), powder	Sigma Aldrich	Cat # F8929
Formalin Solution, Neutral Buffered, 10%	Sigma Aldrich	Cat # HT501128-4L
Gentamycin	Fisher Scientific	Cat # 1405-41-0
HEPES, Liquid	Corning	Cat # MT25060CI
High fat diet	Envigo	Cat # TD.06414
Ionomycin	Sigma-Aldrich	Cat #I0634-5MG
Liberase™ TL Research Grade	Sigma Aldrich	Cat # 5401020001
50 μm Sterile Medicon	BD Bioscience	Cat # 340591
MasterPure™ Yeast DNA Purification Kit	Lucigen	Cat # MPY80200
MEM Nonessential Amino Acid Solution	Corning	Cat # MT25025CI
Monoject 20 mL Syringe	Covidien	Cat # 1182000777

REAGENT or RESOURCE	SOURCE	IDENTIFIER
PCR water	Qiagen	Cat # 17000-10
Penicillin and streptomycin, 100x	Corning	Cat # MT30002CI
Phorbol 12-myristate 13-acetate (PMA)	Sigma-Aldrich	Cat #P8139-10MG
Puritan 6" Sterile Standard Foam Swab w/Polystyrene Handle	Harmony Lab & Safety Supplies	Cat # P25-1506PF-case
HotStarTaq Master Mix Kit	Qiagen	Cat # 203445
RPMI 1640 medium 1X with L-Glutamine	Corning	Cat # MT10040CV
Sabouraud Dextrose Agar, Emmons w/Chloramphenicol	Thermo Scientific	Cat #R01770
Sage 2% Chlorhexidine Gluconate (CHG) Cloths	Medline Industries	Cat # SGE9705
Sabouraud Dextrose Broth	Fisher Scientific	Cat # DF0382-17-9
Sodium Chloride	J. T. Baker	Cat # 3624-01
Sodium Pyruvate 100 mM Solution	Corning	Cat # MT25000CI
TaqMan Fast Advanced Master Mix	Thermo Scientific	Cat # 4444557
Yeast Extract-Peptone-Dextrose (YPD) Broth	BD Bioscience	Cat # 242820
eBioscience Fixation/Permeabilization Concentrate	eBioscience	Cat #00-5123-43
eBioscience Fixation/Permeabilization Diluent	eBioscience	Cat #00-5223-56
eBioscience Permeabilization Buffer (10X)	eBioscience	Cat #00-8333-56
Experimental Models: Organisms/Strains		
Diabetic mice (db/db)	NIAID Taconic Contract	N/A
Rag2$^{-/-}$*Il2rg*$^{-/-}$	NIAID Taconic Contract	Line 111
Rag2$^{-/-}$	NIAID Taconic Contract	Line 103
Il22$^{-/-}$	Dr. Yasmine Belkaid	N/A
Card9$^{-/-}$	Dr. Michail S. Lionakis	N/A
Act1$^{-/-}$	NIAID Taconic Contract	Line 290
Lan-DTA	Dr. Yasmine Belkaid	N/A
C57BL/6 mice	Taconic Biosciences	Cat # B6-F/B6-M
C57BL/10 mice	NIAID Taconic Contract	Line 8411
Oligonucleotides		
CauF 5'-CGCACATTGCGCCTTGGGGTA-3'	Thermo Scientific	N/A
CauR 5'-GTAGTCCTACCTGATTTGAGGCGAC-3'	Thermo Scientific	N/A
Software and Algorithms		
FlowJo v9	Tree Star	https://www.flowjo.com/solutions/flowjo/downloads
GraphPad Prism 4	GraphPad Software	https://www.graphpad.com/scientificsoftware/prism/
R v3.6.0	The R Foundation	https://www.r-project.org/
Other		

REAGENT or RESOURCE	SOURCE	IDENTIFIER
Medimachine	BD Bioscience	Cat # 340588
MediMachine II	Syntec International	Cat # 121600
LSRFortessa	BD Biosciences	https://www.bd.com/en-us/offerings/brands/lsrfortessa
LSR II	BD Biosciences	https://www.bdbiosciences.com/en-us/go-campaign/lsr-ii-comp-cont
QuantStudio 6 Flex	Fisher Scientific	https://www.fishersci.com/shop/products/6-flx96wfast-instlptp-1-system/4485699
GMS staining of mouse ear skin sections	Histoserv	N/A